Supplementary Materials

Targeting and regulating of an Oncogene via Nanovector Delivery of MicroRNA using Patient-Derived Xenografts

Shuyang Sun[1,2#], Yilong Wang[3#], Rong Zhou[1,2], Zicheng Deng[3,4], Yong Han[1,2], Xiao Han[3,4], Wenjie Tao[1,2], Zi Yang[3,4], Chaoji Shi[1,2], Duo Hong[1,2], Jiang Li[1,5], Donglu Shi[3,6*], and Zhiyuan Zhang[1,2*]

1. Department of Oral and Maxillofacial-Head Neck Oncology, Ninth People's Hospital, Shanghai Jiao Tong University, School of Medicine, Shanghai 200011, P. R. China
2. Shanghai Key Laboratory of Stomatology, Shanghai 200011, P. R. China
3. The Institute for Translational Nanomedicine, Shanghai East Hospital, the Institute for Biomedical Engineering & Nano Science, Tongji University School of Medicine, Shanghai 200092, P. R. China
4. School of Materials Science and Engineering, Tongji University, Shanghai 200092, P. R. China
5. Department of Oral Pathology, Ninth People's Hospital, Shanghai Jiao Tong University, School of Medicine, Shanghai 200011, P. R. China
6. The Materials Science and Engineering Program, College of Engineering and Applied Science, University of Cincinnati, Cincinnati, OH 45221, USA

[#] These authors contributed equally.

Corresponding authors: zhzhy@sjtu.edu.cn and donglu.shi@uc.edu

Table S1. Size and zeta potentials of the MMNCs obtained at different PGA/PEI input ratios.

PGA/PEI ratio	Size in DIW, nm	Zeta potential, mV
100:0	273.7	-8.29
45:55	229.8	+14.2
20:80	225.1	+20.6
0:100	1015	+7.28

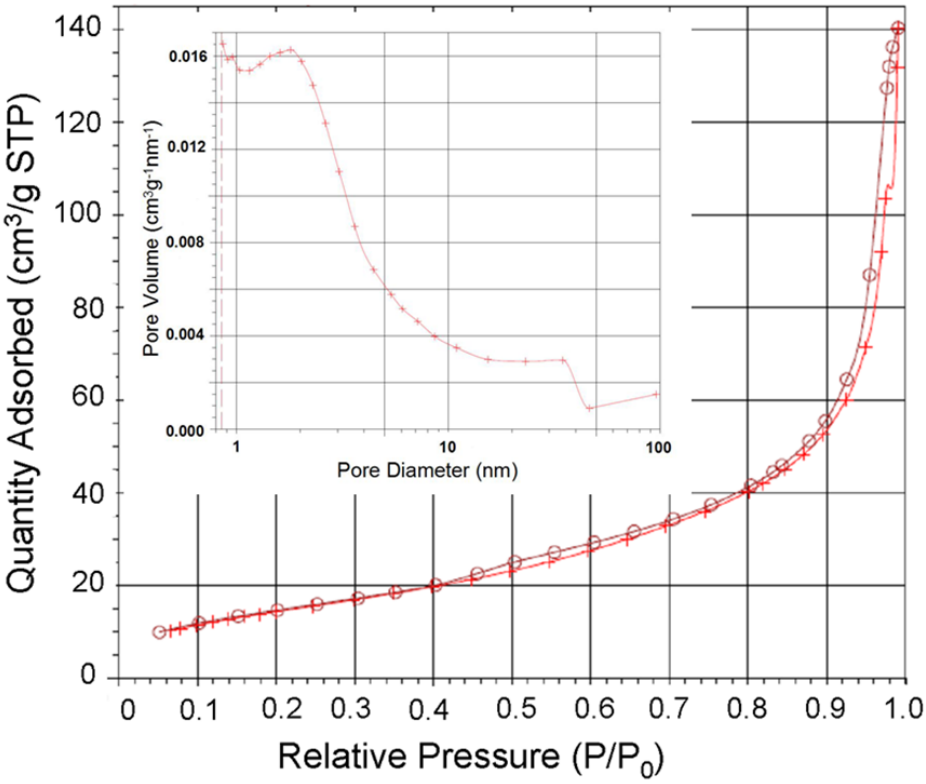

Figure S1. Nitrogen adsorption-desorption isotherms and pore size distribution (inset) of the mesoporous magnetic nanocrystal clusters.

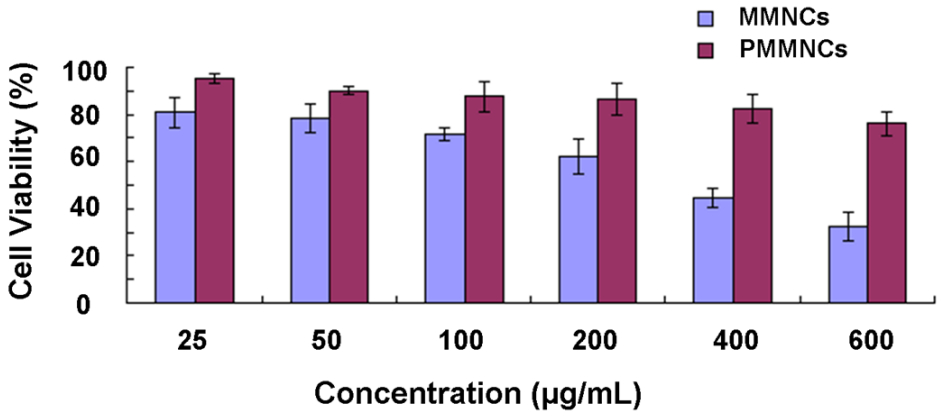

Figure S2. Cytotoxicity of nanoclusters before (MMNCs) and after surface functionalization with PAA molecules (PMMNCs) by MTT assay.

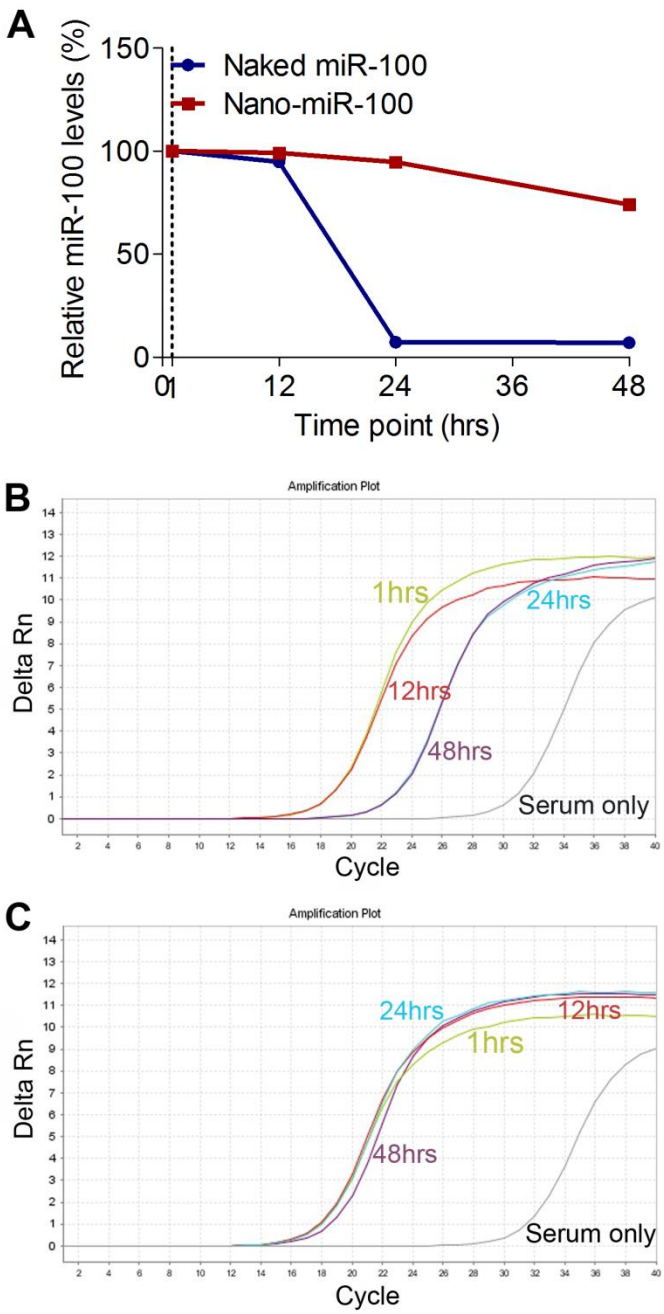

Figure S3. Serum stabilities of naked miR-100 and miR-100 loaded PMMNCs. **(A)** qRT-PCR analysis of relative miR-100 levels in FBS added with either naked or PMMNCs loaded miR-100 at different time points. **(B~C)** Representative original qPT-PCR curves of naked miR-100 (***B***) and PMMNCs-miR-100 (***C***) in FBS at different time points. Delta Rn represents the relative fluorescent signal value.

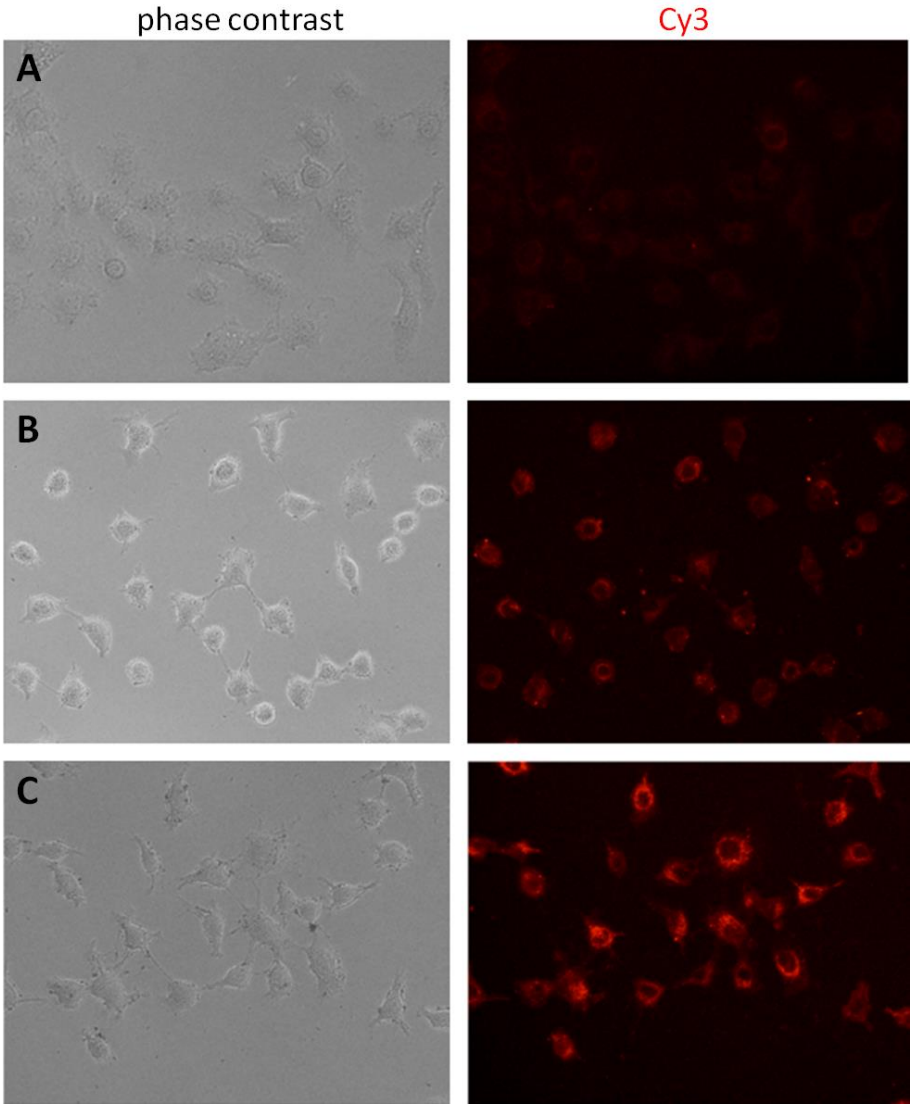

Figure S4. Fluorescent microscopy images of head-and-neck tumor cell lines HN-13 treated with the PMMNCs-miR-100 complex over different times: **(A)** 0.5 hrs, **(B)** 2 hrs, and **(C)** 4 hrs. Original magnification: 20×

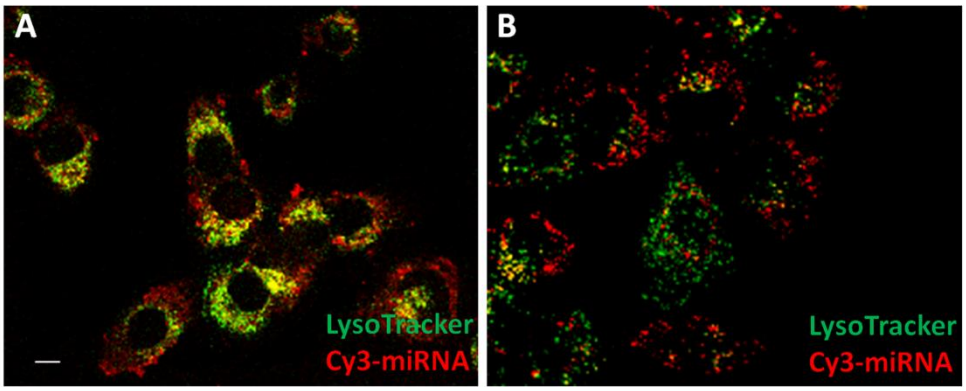

Figure S5. Confocal fluorescence microscopy images of PMMNCs-miR-100 complexes uptake by HN-13 cancer cells at different incubation times: **(A)** 2 hrs and **(B)** 4 hrs. The secondary endosomes and lysosomes (green fluorescence) of HN-13 cells are stained with LysoTracker Green. The miR-100 loaded in PMMNCs is labeled with Cy3 (red fluorescence). The overlay color yellow shows that the complexes are mainly taken up into the lysosomes. Scale bar, 10 μm.

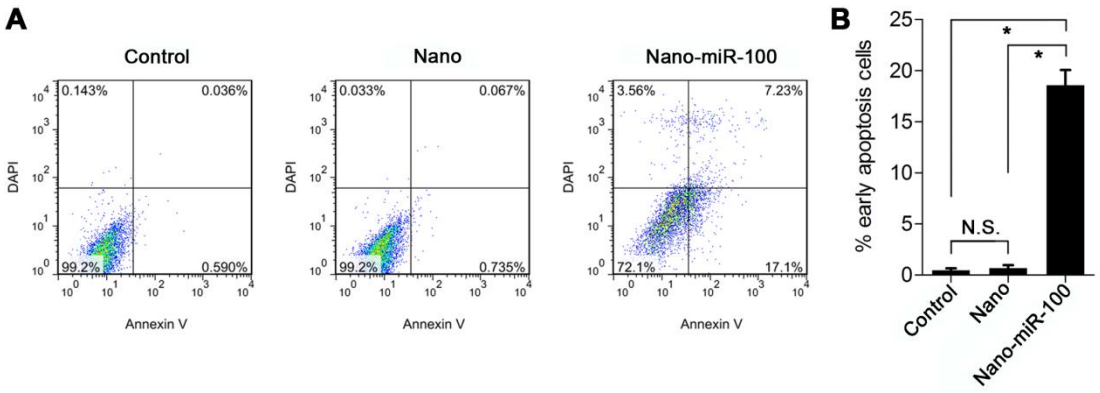

Figure S6. Effects of PMMNCs-miR-100 on cell apoptosis. **(A)** Representative flow cytometric analysis of HN-13 cells treated with blank control, PMMNCs (Nano), or PMMNCs-miR-100 (Nano-miR-100) for 24 hrs. **(B)** Statistical data on the percentage of early apoptotic cells (n=5). All error bars indicate standard deviation. N.S., no statistical signification; *, $p<0.01$ versus control group.

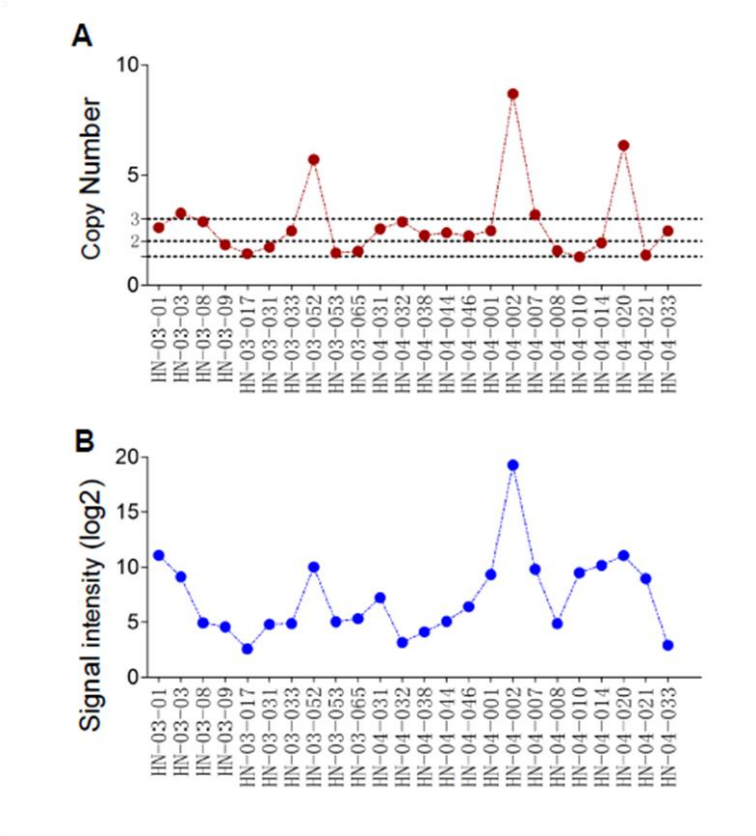

Figure S7. (**A**) Gene copy number of FGFR3 in 24 PDX models. (**B**) mRNA expression levels, represented by signal intensities, of FGFR3 in the 24 PDX models.

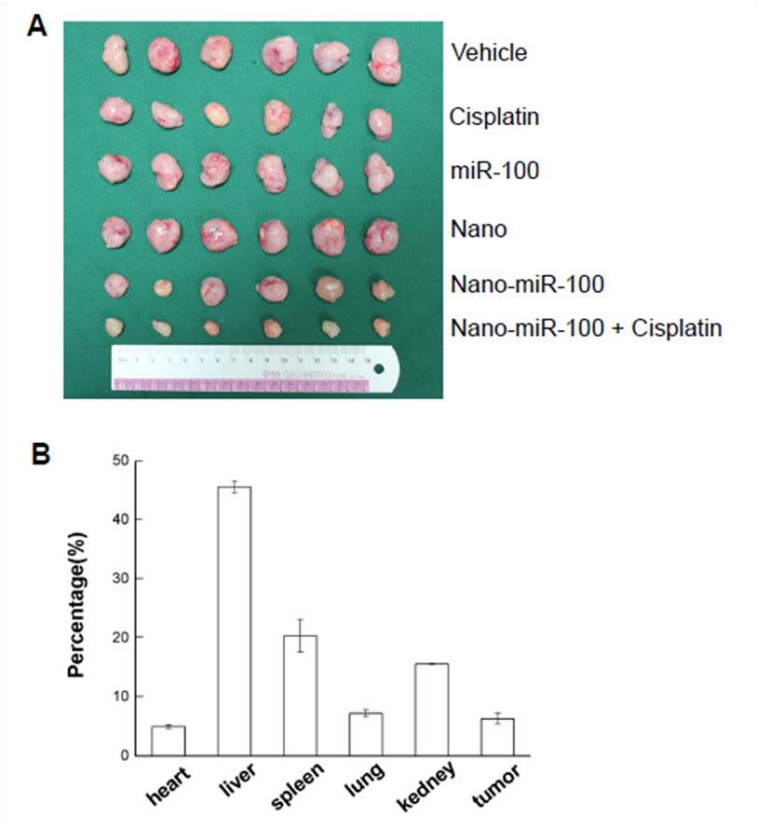

Figure S8. (A) Representative image of HN-04-002 xenograft collected from mice receiving the indicated treatment, 2 hrs after the final treatments. **(B)** The biodistribution of the PMMNCs-miR-100 (nano-miR-100) complex after systemic administration (100 μL each time, 1.0 $mg \cdot mL^{-1}$ nanoparticle content) based on ICP-AES analysis (data expressed as percentage of the injected dose) in the PDX models.